Quantum Oscillations in Flux-Grown SmB_6 with Embedded Aluminum

S. M. Thomas,[1,2] Xiaxin Ding,[3] F. Ronning,[2] V. Zapf,[3] J. D. Thompson,[2] Z. Fisk,[1] J. Xia,[1] and P. F. S. Rosa[2]
[1]Department of Physics and Astronomy, University of California, Irvine, California 92967, USA
[2]Los Alamos National Laboratory, Los Alamos, New Mexico 87545, USA
[3]National High Magnetic Field Laboratory, Los Alamos, New Mexico 87545, USA

(Received 31 May 2018; revised manuscript received 14 September 2018; published 23 April 2019)

SmB_6 is a candidate topological Kondo insulator that displays surface conduction at low temperatures. Here, we perform torque magnetization measurements as a means to detect de Haas–van Alphen (dHvA) oscillations in SmB_6 crystals grown by aluminum flux. We find that dHvA oscillations occur in single crystals containing embedded aluminum, originating from the flux used to synthesize SmB_6. Measurements on a sample with multiple, unconnected aluminum inclusions show that aluminum crystallizes in a preferred orientation within the SmB_6 cubic lattice. The presence of aluminum is confirmed through bulk susceptibility measurements, but does not show a signature in transport measurements. We discuss the ramifications of our results.

DOI: 10.1103/PhysRevLett.122.166401

Single crystalline SmB_6 has been studied since the 1970s, but many mysteries still remain. SmB_6 was initially viewed as a prototypical Kondo insulator, in which incoherent scattering from f electrons occurs at high temperatures whereas an insulating gap—driven by the hybridization between f states and d conduction bands—opens at low temperatures [1]. Further, a puzzling resistance saturation near 4 K was dismissed as arising from in-gap impurity states [2], but theoretical models recently suggested that SmB_6 is a topological Kondo insulator with conductive surface states and a robust bulk gap [3,4]. Thickness-dependent transport measurements in crystals grown via aluminum flux have shown that the resistance plateau is due to a metallic surface state surrounding the insulating bulk [5,6]. Recent inverted Corbino measurements on the same crystals show that the bulk of SmB_6 displays a 10 order of magnitude increase in resistance with decreasing temperature, indicating that the bulk is truly insulating [7]. Nonetheless, SmB_6 grown by the floating-zone method was claimed to host an exotic bulk Fermi surface (FS) in an insulating state [8].

Direct evidence of the expected topological helical structure of the surface states in SmB_6, however, remains elusive, and probes other than electrical transport are imperative. Spin-dependent angle-resolved photoemission spectroscopy (ARPES), which provides information on the band dispersion near the FS, was an obvious first choice. ARPES experiments in SmB_6 have revealed in-gap states [9–11], but issues with spin-resolved ARPES resolution compared to the small hybridization gap have made direct observation of spin-momentum locking in the surface states challenging and controversial [11–13].

Further information about the FS can be obtained through quantum oscillation measurements, via angular dependent measurements of the extremal areas [14]. Although quantum oscillations have not been observed in the dc electrical resistivity of SmB_6, two independent reports have been made on de Haas–van Alphen oscillations (dHvA, i.e., oscillations in the magnetization). In the first report, dHvA oscillations in flux-grown crystals were attributed to a two-dimensional (2D) FS arising from the metallic surface state [15]. Contrary to claims of a heavy effective mass observed in studies using thermopower and scanning tunneling spectroscopy [16,17], the cyclotron mass extracted from these dHvA measurements was found to be on the order of $0.1m_e$. Considering the high mobility and light mass, it is remarkable that experimental evidence of oscillations has not been found in transport measurements. Further, the origin of the surface state was thought to be the hybridization between the conduction band and the heavy Sm f electrons, which also suggests a heavy surface state. In the second report of quantum oscillations, the measured FS in floating-zone-grown crystals was claimed to have three-dimensional (3D) shape and to arise from the insulating bulk states [8]. This result is also unexpected considering that quantum oscillations are traditionally observed in clean, metallic systems. Because of these reports, numerous theoretical explanations have been reported for both the light electrons observed in the 2D FS [18], and for the presence of oscillations arising from an insulating state [19–28].

To shed light on this controversy, here we use torque magnetometry [29] to measure quantum oscillations in the magnetization of flux-grown SmB_6 as a function of its thickness. We find that flux-grown crystals only exhibit dHvA oscillations when embedded aluminum is present. The Al inclusions co-crystallize with the SmB_6 host crystal, with the [100] Al axis nearly aligned with the [100] SmB_6 axis. Angular dependence of our dHvA oscillations is in

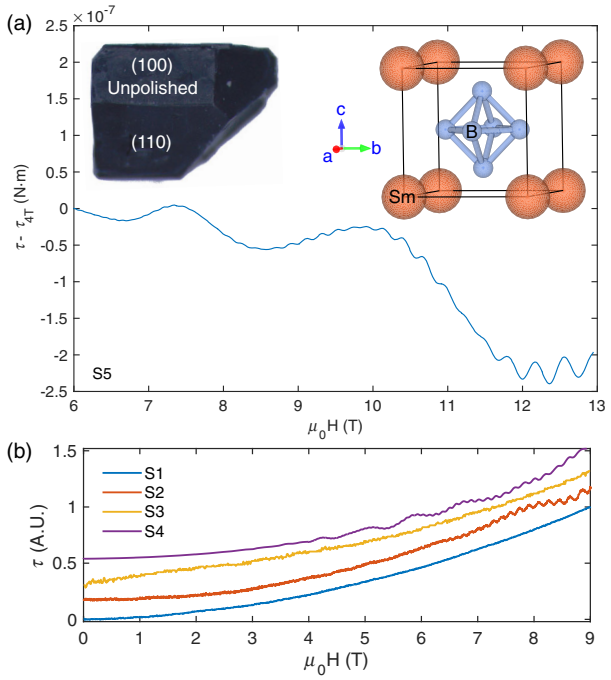

FIG. 1. (a) Torque magnetization as a function of magnetic field of a representative SmB_6 single crystal (s5). To focus on the oscillations, the value of the torque at 4 T was subtracted from the data. The inset shows a picture of the as-grown sample along with its cubic crystal structure. (b) A survey of several SmB_6 crystals that were checked for quantum oscillations using torque magnetometry. Only samples s2 and s4 showed oscillations.

good agreement with those reported previously for single crystalline Al [30–32]. Interestingly, Al inclusions in the bulk show no evidence for a superconducting transition in transport measurements.

For our investigation, we choose single crystals of SmB_6 grown using the aluminum flux technique [33]. The inset of Fig. 1(a) shows a typical flux-grown crystal of SmB_6 with dimensions $3 \times 2 \times 1$ mm^3. Aluminum does not substitute into the hexaboride lattice, but larger crystals often enclose Al pockets, which can be mechanically removed by polishing or chemically etched with hydrochloric acid. We note that Al also crystallizes in a cubic space group, $Fm\text{-}3m$ (225), with a lattice parameter $a = 4.05$ Å that is only 2% smaller than that of SmB_6.

Quantum oscillations arise in many physical properties of metallic materials under the condition that $\omega_c\tau > 1$, where ω_c is the cyclotron frequency and τ is the electron scattering time. Onsager showed that the oscillation period in inverse field is proportional to the cross-sectional area of the FS [37]:

$$\Delta\left(\frac{1}{B}\right) = \frac{2\pi e}{\hbar}\frac{1}{A_e}. \tag{1}$$

For a 2D material, the FS is expected to have cylindrical character. The oscillation frequency for a [001] rotation axis should vary as $1/\cos(\theta - \phi_S)$, where θ is the angle between [100] and the field and ϕ_S is the angle between a surface normal and [100]. Because SmB_6 crystals grow with (100) and (110) facets, surface states on these facets should have $\phi_S = 90n$ and $\phi_S = 45 + 90n$ degrees, respectively, where n is an integer. In a 3D material, the frequency will also diverge along any open orbits.

In an attempt to determine the nature of the quantum oscillations in SmB_6, torque magnetometry measurements were performed on many flux-grown single crystals either as-grown or polished. As shown in Fig. 1(b), however, only a subset of SmB_6 samples showed oscillatory behavior in magnetization. These samples tended to have larger thickness, but no correlation was observed with surface condition (i.e., as grown versus polished). The lack of oscillations in some of the samples, despite having similar surface facets and surface area, was the first indication that the presence of oscillations may not be intrinsic to the metallic surface state of SmB_6 crystals. As shown in the Supplemental Material, magnetoresistance at 50 mK was also measured in one of the samples that showed dHvA oscillations. After subtracting a polynomial background, the frequency content of the magnetoresistance was calculated. The lack of any clear peak in the frequency spectrum shows that Shubnikov–de Haas (SdH) oscillations are not detectable in fields to 12 T, even at 50 mK [33]. This result is consistent with a magnetoresistance study on SmB_6 at temperatures as low as 300 mK using special contact structures to only measure the contribution from individual crystal surfaces [38].

One of the crystals exhibiting dHvA oscillations [s5, Fig. 1(a)] was polished to determine the origin of the quantum oscillations. Only the bottom surface was polished, and care was taken to keep the top surface shown in Fig. 1(a) intact. After each polishing step, any exposed aluminum was etched away using hydrochloric acid. Polishing was necessary between etching steps because only visible aluminum will be exposed to the etchant. As shown in the left inset of Fig. 2(a), three disconnected aluminum inclusions appeared after polishing away the bottom portion of the crystal. After further polishing, several more unconnected inclusions were discovered, one of which is shown in the middle inset of Fig. 2(a). At the end, the sample was polished to 230 microns and no Al inclusions were apparent [Fig. 2(a), right inset].

Figure 2(a) shows the torque magnetization obtained in the as-grown sample ($m = 21.6$ mg) compared to the signal obtained after polishing away roughly half of the sample ($m = 11.3$ mg). Remarkably, frequency analysis shown in Fig. 2(b) revealed that the FFT amplitude roughly scales with the mass of the sample and not the sample area—consistent with oscillations arising from Al inclusions that are distributed in the bulk of the crystal. Moreover, well-defined peaks exhibiting clear angular dependence are observed in the frequency spectrum, despite the presence of multiple aluminum inclusions.

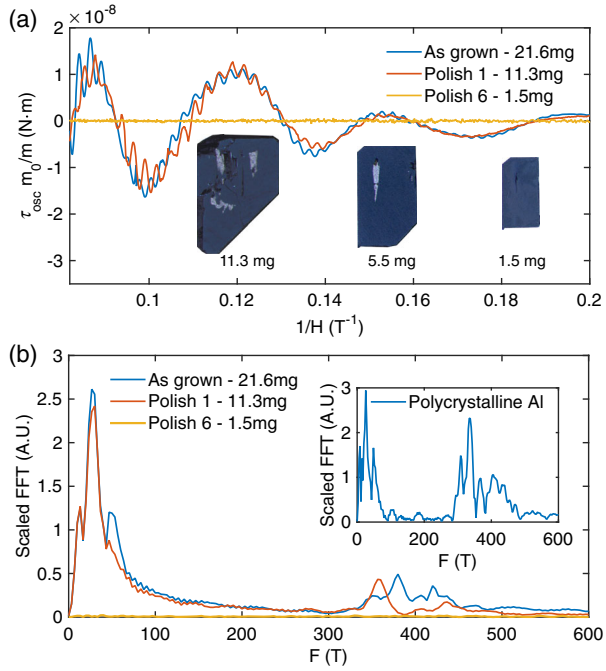

FIG. 2. (a) Oscillatory torque versus inverse field for s5 at several different polishing steps. The torque is scaled with the mass of the sample (m_0/m), and field is applied a few degrees from [010]. After the last aluminum deposit is removed, the oscillations vanish. The inset pictures show progressive polishing of sample s5, depicting a series of aluminum deposits distributed throughout the sample. The initial (100) surface was left undisturbed. (b) Frequency spectra of the oscillatory torque shown above. The spectra are scaled by the mass of the sample (m_0/m). Inset shows frequency spectrum of polycrystalline Al flux. There is broad spectral weight between 300 and 500 T, in contrast to the oriented single-crystal aluminum in flux-grown SmB_6.

In contrast, the inset of Fig. 2(b) shows dHvA oscillations from a small piece of 5N aluminum used as flux during the growth process. There are more than five peaks in the 300–500 T range due to the fact that the pellet is composed of many randomly oriented microcrystals. Further, polycrystalline Al does not exhibit a clear pattern in angle-dependent measurements [15]. Considering the multitude of distinct aluminum inclusions in this particular SmB_6 crystal, the relatively sparse spectrum with well-defined angular dependence shows that the inclusions are preferentially aligned along the same crystallographic axis. The fact that embedded aluminum inclusions co-crystallize with the SmB_6 was also reported in a study combining neutron diffraction, powder diffraction, and x-ray computed tomography [39].

To check that the sole source of the oscillations was embedded aluminum deposits, the sample was polished to a thin plate as shown in the right inset of Fig. 2(a). As shown in Fig. 2, there are no oscillations observed after the final polish and etching step, even though the (100) surface on the top of the sample has been left undisturbed. This confirms that the source of the observed oscillations is the embedded Al deposits in SmB_6.

Having established the origin of the dHvA signal in flux-grown SmB_6, we now briefly turn to the temperature dependence and angle dependence of the oscillations. The magnitude of the dHvA oscillations follows the temperature dependence given by the Lifshitz-Kosevich formula [14]:

$$R_T = \alpha T m^*/B \sinh(\alpha T m^*/B). \quad (2)$$

A fit of the 288 T oscillation amplitude with field applied 45° from [100] gives an effective mass of $0.133 m_e$ (see Supplemental Material, Sec. VI [33]). This angle was chosen because it provides the largest separation of the oscillations in frequency. The effective mass agrees with a previous report on single-crystal aluminum that found a value of $0.130(4) m_e$ for field along the same direction [30].

Figures 3(c)–3(d) shows the angular dependence of the dHvA oscillations in SmB_6 as the crystal is rotated about the [001] axis. The pockets with minimum frequency near 375 T were labeled α pockets, whereas those with minimum frequency near 290 T were labeled β pockets. The observed oscillation frequencies compare well with those for single-crystal aluminum as reported by Larson *et al.* [30,40]. The authors measured single-crystal Al from [010] to [110] rotating in the (100) plane and assigned four pocket designations (γ_{1-4}) for frequencies in the 200–1000 T range. Because Al is fourfold symmetric in the (100) plane, these designations are actually two pockets that repeat every 90°. γ_1 and γ_3 correspond to a pocket with minimum oscillation near 285 T, and γ_2 and γ_4 correspond to a pocket with minimum oscillation near 390 T. This remarkable similarity further confirms our scenario that the [001] axis of the aluminum inclusions in SmB_6 is very nearly aligned with the SmB_6 [001] axis.

The small difference at larger angles may be attributed to the presence of small amounts of strain due to the 0.08 Å mismatch in lattice parameters between Al and SmB_6. Fits to the expected angular dependence of a 2D FS, $F_0/\cos(\theta - \phi_S)$, are also shown for comparison. Lastly, the angular dependence was also measured after etching the three aluminum deposits depicted in Fig. 2(a) (left inset). Removing nearly half of the embedded aluminum had little effect on the angular dependence of the observed oscillations [Figs. 3(c)–3(d), open symbols]. Again, this demonstrates that the Al inclusions are co-aligned.

Aluminum has a superconducting critical temperature of 1.17 K and a critical field of 105 Oe [41]. Figure 3(a) shows transport measurements performed on a SmB_6 crystal near the superconducting transition of Al. Remarkably, no feature is visible in resistivity. Down to 2 K, the bulk of flux-grown SmB_6 is insulating as shown recently by Eo *et al.*, which explains the lack of SdH oscillations in SmB_6 or transport evidence of the superconducting

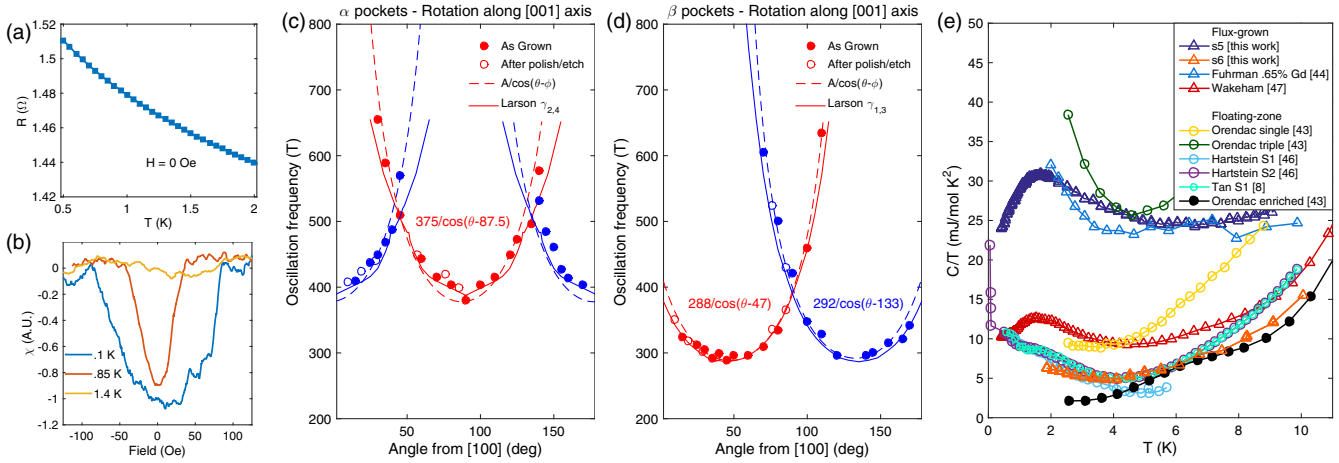

FIG. 3. (a) Resistance versus temperature in zero applied field for a SmB_6 crystal with a subsurface aluminum inclusion. (b) ac susceptibility measurement of SmB_6 crystal near zero field. (c) Angular dependence of the dHvA oscillation frequency for the α pocket. (d) Angular dependence of the dHvA oscillation frequency for the β pocket. (e) Low temperature specific heat reported in the literature for SmB_6. Numbers in brackets indicate citation.

transition from subsurface Al inclusions [7]. In contrast, subsurface aluminum can be detected through bulk magnetization measurements. As shown in Fig. 3(b), the aluminum superconducting transition is visible in ac susceptibility measurements [42].

After these transport and susceptibility measurements, the sample was polished to determine the proximity of the Al inclusions to the surface. Subsurface Al deposits became visible after only a few polishing laps, showing that the inclusion was separated from the surface by less than 100 μm. Because of the highly insulating bulk in SmB_6 at low temperatures, an aluminum inclusion that is shallowly embedded within the bulk is completely isolated from the metallic surface state. Thus, when screening SmB_6 samples for aluminum inclusions, resistance measurements are insufficient.

Heat capacity is also an illuminating bulk thermodynamic probe. Figure 3(e) shows a comparison of low-temperature heat capacity in SmB_6 collected from several studies reported in the literature. The first notable aspect is the great variation of the residual heat capacity of both floating-zone and flux-grown samples. The lowest heat capacity was seen in a sample grown with enriched Sm and B [43], providing evidence that the broad feature centered near 1.5 K is caused by naturally occurring impurities. The 0.65% Gd-doped sample reported by Fuhrman *et al.*, has the largest rise of any flux-grown sample show in Fig. 3(e), and higher values were observed as the Gd impurities were increased [44]. Importantly, recent scanning tunneling microscopy experiments in Gd-doped SmB_6 reveal that small amounts of Gd (<3%) act locally and do not percolate [45]. This explains why small amounts of impurities affect heat capacity but not dc electrical resistivity. Accordingly, we stress that there is no relation between low-temperature heat capacity and the presence of quantum oscillations in flux-grown samples. We found no quantum oscillations in the sample with the lowest residual heat capacity (s6, see Supplemental, Sec. IV [33]) after Al inclusions were removed. This again attests that Al is the sole source of quantum oscillations in flux-grown SmB_6.

We also stress that the results reported here primarily focus on flux-grown crystals. A more recent report on the 3D FS in floating-zone samples also includes data from flux-grown samples with low-temperature heat capacity similar to that reported by Wakeham *et al.* [46,47], but the angular dependence of the quantum oscillations indicates that the samples used in the study also contain embedded Al (see Supplemental, Sec. II [33]). In contrast, floating-zone samples exhibiting quantum oscillations are known to have an anomalous increase in specific heat and oscillation amplitude at very low temperatures ($T \leq 1$ K) [8,46]. If this is an intrinsic property of stoichiometric SmB_6, its absence in flux-grown samples must be understood. Many different theories have been proposed for the origin of the quantum oscillations in floating-zone samples [19–22,25–27], but enlightened by our results, we deem important to discuss the possibility that quantum oscillations could arise in correlated narrow-gap materials in the presence of disorder [23,24,28].

Orendac *et al.* show that as the number of zone refinements is increased the residual heat capacity also increases [43]. This is attributed to an increase in the number of Sm vacancies, which are expected to be more prevalent in floating-zone samples due to the refinement temperature being higher than the boiling point of Sm. A larger number of Sm vacancies in floating-zone samples has been also detected by Raman spectroscopy measurements [48]. All floating-zone samples in which quantum oscillations were observed, however, have strikingly similar low-temperature

heat capacity, with magnitudes much lower than the triply refined sample reported by Orendac *et al.* [dark green circles in Fig. 3(e)] [8,43,46]. This result suggests that Sm vacancies (i.e., point defects) alone may not be the cause of quantum oscillations. Nevertheless, we emphasize that floating-zone crystals are grown at temperatures higher than 2000 °C which, combined with the tendency of borides to form defects, may cause other crystallographic imperfections such as linear defects (e.g., dislocations) and planar defects (e.g., grain boundaries and stacking faults). The possibility that crystallographic defects in floating-zone SmB_6 crystals play a role similar to Al impurities in flux-grown crystals is worth investigating.

In conclusion, we have shown that dHvA oscillations in flux-grown SmB_6 arise from subsurface aluminum inclusions. The inclusions are nearly aligned with the SmB_6 [001] crystal axis and provide quantum oscillations with an effective mass of $0.1m_e$. After completely removing all aluminum inclusions, the dHvA oscillation signal vanishes. Angular dependence shows that the orbits are in good agreement with those of single crystalline Al in previous reports [30,32]. Our results demonstrate that, when performing measurements on SmB_6 crystals, it is necessary to screen the samples for aluminum by using a bulk technique capable of probing beyond the metallic surface state. The absence of quantum oscillations in flux-grown SmB_6 imposes strong constraints to the understanding of quantum oscillation phenomena in Kondo insulators.

We would like to acknowledge constructive discussions with Y. S. Eo, W. Fuhrman, T. M. McQueen, and C. Kurdak. Work at Los Alamos was performed under the auspices of the U.S. Department of Energy, Office of Basic Energy Sciences, project "Quantum Fluctuations in Narrow Band Systems". S. M. T. acknowledges support from the Los Alamos Laboratory Directed Research and Development program under Project No. 20160085DR. Work at U.C.I. was supported by NSF Grant No. DMR-1708199. A portion of this work was performed at the National High Magnetic Field Laboratory, which is supported by National Science Foundation Cooperative Agreement No. DMR-1157490 and by the U.S. Department of Energy, Office of Basic Energy Sciences, project "Science of 100 Tesla".

[1] Z. Fisk, J. Sarrao, S. Cooper, P. Nyhus, G. Boebinger, A. Passner, and P. Canfield, Physica B (Amsterdam) **223–224B**, 409 (1996).
[2] A. Menth, E. Buehler, and T. H. Geballe, Phys. Rev. Lett. **22**, 295 (1969).
[3] M. Dzero, K. Sun, V. Galitski, and P. Coleman, Phys. Rev. Lett. **104**, 106408 (2010).
[4] T. Takimoto, J. Phys. Soc. Jpn. **80**, 123710 (2011).
[5] D. J. Kim, S. Thomas, T. Grant, J. Botimer, Z. Fisk, and J. Xia, Sci. Rep. **3**, 3150 (2013).
[6] S. Wolgast, Ç. Kurdak, K. Sun, J. W. Allen, D.-J. Kim, and Z. Fisk, Phys. Rev. B **88**, 180405(R) (2013).
[7] Y. S. Eo, A. Rakoski, J. Lucien, D. Mihaliov, C. Kurdak, P. F. S. Rosa, D.-J. Kim, and Z. Fisk, arXiv:1803.00959.
[8] B. S. Tan, Y.-T. Hsu, B. Zeng, M. C. Hatnean, N. Harrison, Z. Zhu, M. Hartstein, M. Kiourlappou, A. Srivastava, M. D. Johannes *et al.*, Science **349**, 287 (2015).
[9] N. Xu, X. Shi, P. K. Biswas, C. E. Matt, R. S. Dhaka, Y. Huang, N. C. Plumb, M. Radović, J. H. Dil, E. Pomjakushina *et al.*, Phys. Rev. B **88**, 121102(R) (2013).
[10] J. Jiang, S. Li, T. Zhang, Z. Sun, F. Chen, Z. Ye, M. Xu, Q. Ge, S. Tan, X. Niu *et al.*, Nat. Commun. **4**, 3010 (2013).
[11] M. Neupane, N. Alidoust, S.-Y. Xu, T. Kondo, Y. Ishida, D. J. Kim, C. Liu, I. Belopolski, Y. J. Jo, T.-R. Chang *et al.*, Nat. Commun. **4**, 2991 (2013).
[12] P. Hlawenka, K. Siemensmeyer, E. Weschke, A. Varykhalov, J. Sánchez-Barriga, N. Y. Shitsevalova, A. V. Dukhnenko, V. B. Filipov, S. Gabáni, K. Flachbart *et al.*, Nat. Commun. **9**, 517 (2018).
[13] C. E. Matt, H. Pirie, A. Soumyanarayanan, M. M. Yee, Y. He, D. T. Larson, W. S. Paz, J. J. Palacios, M. H. Hamidian, and J. E. Hoffman, arXiv:1810.13442.
[14] D. Shoenberg, *Magnetic Oscillations in Metals* (Cambridge University Press, Cambridge, England, 1984).
[15] G. Li, Z. Xiang, F. Yu, T. Asaba, B. Lawson, P. Cai, C. Tinsman, A. Berkley, S. Wolgast, Y. S. Eo *et al.*, Science **346**, 1208 (2014).
[16] Y. Luo, H. Chen, J. Dai, Z.-a. Xu, and J. D. Thompson, Phys. Rev. B **91**, 075130 (2015).
[17] H. Pirie, Y. Liu, A. Soumyanarayanan, P. Chen, Y. He, M. M. Yee, P. F. S. Rosa, J. D. Thompson, D.-j. Kim, Z. Fisk *et al.*, arXiv:1810.13419.
[18] V. Alexandrov, P. Coleman, and O. Erten, Phys. Rev. Lett. **114**, 177202 (2015).
[19] J. Knolle and N. R. Cooper, Phys. Rev. Lett. **115**, 146401 (2015).
[20] O. Erten, P. Ghaemi, and P. Coleman, Phys. Rev. Lett. **116**, 046403 (2016).
[21] O. Erten, P.-Y. Chang, P. Coleman, and A. M. Tsvelik, Phys. Rev. Lett. **119**, 057603 (2017).
[22] H. K. Pal, Phys. Rev. B **99**, 045149 (2019).
[23] H. Shen and L. Fu, Phys. Rev. Lett. **121**, 026403 (2018).
[24] N. Harrison, Phys. Rev. Lett. **121**, 026602 (2018).
[25] D. Chowdhury, I. Sodemann, and T. Senthil, Nat. Commun. **9**, 1766 (2018).
[26] L. Zhang, X.-Y. Song, and F. Wang, Phys. Rev. Lett. **116**, 046404 (2016).
[27] G. Baskaran, arXiv:1507.03477.
[28] W. T. Fuhrman and P. Nikolić, arXiv:1807.00005.
[29] R. Griessen, Cryogenics **13**, 375 (1973).
[30] C. O. Larson and W. L. Gordon, Phys. Rev. **156**, 703 (1967).
[31] P. T. Coleridge and P. M. Holtham, J. Phys. F **7**, 1891 (1977).
[32] C. M. Boyne and L. Mackinnon, J. Phys. F **8**, 629 (1978).
[33] See Supplemental Material at http://link.aps.org/supplemental/10.1103/PhysRevLett.122.166401, Sec. I includes details on sample growth, which includes Refs. [34,35]. Section III shows that SdH oscillations were observed when leads were attached directly to an exposed Al inclusion, which includes Ref. [36].

[34] Z. Fisk and J. P. Remeika, *Handbook on the Physics and Chemistry of Rare Earths* (Elsevier, Amsterdam, 1989), Vol. 12.
[35] Z. Fisk, A. Lawson, and R. Fitzgerald, Mater. Res. Bull. **9**, 633 (1974).
[36] J. P. G. Shepherd and W. L. Gordon, Phys. Rev. **169**, 541 (1968).
[37] L. Onsager, Philos. Mag. Ser. 5 **43**, 1006 (1952).
[38] S. Wolgast, Y. S. Eo, T. Öztürk, G. Li, Z. Xiang, C. Tinsman, T. Asaba, B. Lawson, F. Yu, J. W. Allen *et al.*, Phys. Rev. B **92**, 115110 (2015).
[39] W. A. Phelan, S. M. Koohpayeh, P. Cottingham, J. A. Tutmaher, J. C. Leiner, M. D. Lumsden, C. M. Lavelle, X. P. Wang, C. Hoffmann, M. A. Siegler *et al.*, Sci. Rep. **6**, 20860 (2016).
[40] E. M. Gunnersen, Phil. Trans. R. Soc. A **249**, 299 (1957).
[41] S. Caplan and G. Chanin, Phys. Rev. **138**, A1428 (1965).
[42] S. C. Whitmore, S. R. Ryan, and T. M. Sanders, Rev. Sci. Instrum. **49**, 1579 (1978).
[43] M. Orendáč, S. Gabáni, G. Pristáš, E. Gažo, P. Diko, P. Farkašovský, A. Levchenko, N. Shitsevalova, and K. Flachbart, Phys. Rev. B **96**, 115101 (2017).
[44] W. T. Fuhrman, J. R. Chamorro, P. A. Alekseev, J.-M. Mignot, T. Keller, J. A. Rodriguez-Rivera, Y. Qiu, P. Nikolić, T. M. McQueen, and C. L. Broholm, Nat. Commun. **9**, 1539 (2018).
[45] L. Jiao, S. Rößler, D. Kasinathan, P. F. S. Rosa, C. Guo, H. Yuan, C.-X. Liu, Z. Fisk, F. Steglich, and S. Wirth, Sci. Adv. **4**, eaau4886 (2018).
[46] M. Hartstein, W. H. Toews, Y.-T. Hsu, B. Zeng, X. Chen, M. C. Hatnean, Q. R. Zhang, S. Nakamura, A. S. Padgett, G. Rodway-Gant *et al.*, Nat. Phys. **14**, 166 (2018).
[47] N. Wakeham, P. F. S. Rosa, Y. Q. Wang, M. Kang, Z. Fisk, F. Ronning, and J. D. Thompson, Phys. Rev. B **94**, 035127 (2016).
[48] M. E. Valentine, S. Koohpayeh, W. A. Phelan, T. M. McQueen, P. F. S. Rosa, Z. Fisk, and N. Drichko, Phys. Rev. B **94**, 075102 (2016).